Internal Gravity Wave Activity Hotspot and Implications for the Middle Atmospheric Dynamics

Petr Sacha[1], Petr Pisoft[1], Ales Kuchar[1], Friederike Lilienthal[2] and Christoph Jacobi[2]

[1]Department of Atmospheric Physics, Faculty of Mathematics and Physics, Charles University in Prague, Prague, Czech Republic, petr.sacha@mff.cuni.cz;

[2]Institute for Meteorology, University of Leipzig, Stephanstr. 3, D-04103 Leipzig, Germany

Abstract: The Internal gravity waves are widely recognized to contribute significantly to the energy and angular momentum transport. They play significant role in affecting many of the middle atmospheric phenomena (like QBO or Brewer-Dobson circulation). Using the GPS RO density profiles, we have discovered a localized area of enhanced IGW activity and breaking in the lower stratosphere of Eastern Asia/North-western Pacific region. With a mechanistic model for the middle atmosphere we studied the effects of such a localized breaking region on a large-scale dynamics and transport. Possible formation and propagation directions of planetary waves caused by such a localized forcing were investigated and consequences for the polar vortex stability and stratosphere-troposphere exchange in the tropical region were discussed. Finally, applying 3D EP flux and 3D residual circulation diagnostics, we investigated possible role of this area in longitudinal variability of the Brewer-Dobson circulation with a hypothesis of its enhanced downwelling branch in this region. In the proces, model results were compared with the ozone and tracer distribution data from GOME, GOMOS, MIPAS and SCIAMACHY instruments further confirming the importance of the Eastern Asia/North-western Pacific region for middle atmospheric dynamics.

Methodology

- L2 level FORMOSAT-3/COSMIC GPS RO density profiles (Šácha et al., 2014) on a 3° × 3° grid ranging from tropopause up to 35 km and from 2007 to 2010
- The potential energy density of disturbances per unit mass (Ep) as a proxy for IGWactivity was computed using the formula provided by Wilson et al. (1991).

$$Ep = \frac{1}{2}N^2\langle\xi^2\rangle = \frac{1}{2}\left(\frac{g}{N}\right)^2\left\langle\left(\frac{\rho'}{\rho_0}\right)^2\right\rangle$$

- To access the stability of the wave field:
  - Dynamical instability – gradient Richardson number estimated by Senft and Gardner (1991):
    $$Ri_g = \frac{g^2}{N^4}\left\langle\left[\frac{\partial}{\partial z}\left(\frac{\rho'}{\rho_0}\right)\right]^2\right\rangle$$
  - Rayleigh-Taylor convective instability - Sutherland (2008) a maximum growth rate of disturbances:
    $$\sigma^2 = \frac{g}{\rho_0}\left(\frac{d\bar{\rho}}{dz} + \frac{\partial\rho'}{\partial z}\right)$$
- Multi Sensor Reanalysis of Ozone (MSR) total ozone column field from 1978 to 2008. Data from TOMS (on the satellites Nimbus-7 and Earth Probe), SBUV (Nimbus-7, AA-9, NOAA-11 and NOAA-16), GOME (ERS-2), SCIAMACHY (Envisat), OMI (EOS-Aura), and GOME-2 (Metop-A). Producer- KNMI.
- 3D assimilated nadir ozone profiles from GOME and GOME-2 observations developed within the ozone project of the CCI programme of ESA. Producer- KNMI.
- N_2O, CO, H_2O volume mixing ratio profiles from MIPAS V5R data. Producer - KIT IMK/IAA.

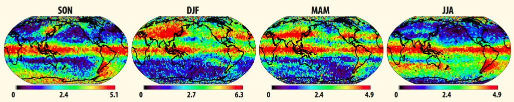

Figure 1. Seasonal means of the potential energy in J/kg averaged across the whole vertical profile for the studied time period 2007-2010.

Results I

Analysis of geographical and seasonal distribution of IGW activity and effects

- Distribution of potential energy of disturbances: In average, a distinguished region of high IGW activity and of maximal values in the Northern Hemisphere in October and November (see Figure 1). This area is significant starting from the 70 hPa level up to the 6 hPa level.
- Wave breaking indication: Richardson number and convective instability growth rate values and distributions are further accentuating the importance of our area making it a dominant feature of the maps across all the levels even in spring and winter months and being suggestive of vertically robust and long lasting breaking of IGWs (See Figures 2 and 3).
- Possible wave sources
  - Convective activity connected with the Kuroshio current in autumn.
  - Low values of cumulative wind rotation above our region are favorable for vertical propagation of orographic waves (c_p=0).
  - Surface winds suggestive of orographic creation of IGW due to the topography of Japan, Sachalin, Korean Peninsula and eastern Asia coastline.
  - In situ wave generation in the upper troposphere/lower stratosphere (Mohri (1953) – subtropical and polar jet stream merging)

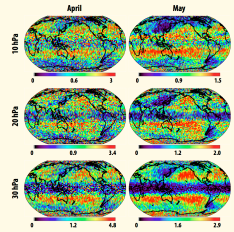

Figure 2. Selected monthly means of the gradient Richardson number at 10, 20 and 30 hPa.

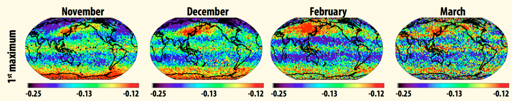

Figure 3. Selected monthly means of selected (secondary) sigma maxima in s^{-2} for the studied time period 2007-2010.

Results II

Longitudinal variability of BDC and planetary waves sourcing

- MUAM 3D mechanistic circulation model (Pogoreltsev et al., 2007) runs with IGW parameterization input based on geographical distribution of wave activity from GPS RO
- In comparison with the reference run for January – 2D Eliassen-Palm flux analysis reveals in the LS stronger planetary wave propagation from midlatitudes equatorward and at the edge of polar vortex (Fig. 4).
- 3D analysis reveals enhanced downwelling above NP/EA region penetrating to lower levels than elsewhere.
- Robustness of the enhanced BDC branch occurence above NP/EA region and modeled vertical residual circulation distribution is confirmed by the 30 year average of total ozone column in January (Fig. 6), where the maximum is located in this region.

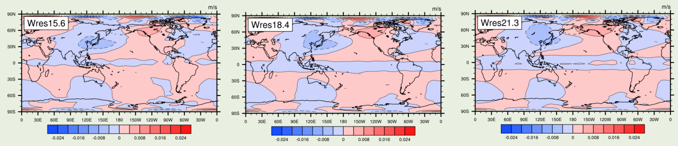

Figure 5. Geographical distribution of the residual vertical velocity (Kinoshita and Sato, 2013) on three consequent model levels in the LS region

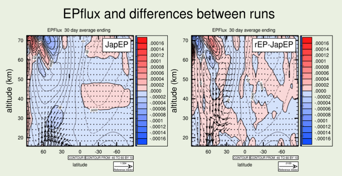

Figure 4. Left: Mean E-P flux and its divergence from GPS RO based IGW weights run for January conditions, contours show mean zonal wind. Right: Difference between reference and GPS RO based run.

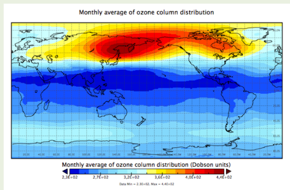

Fig. 6: Mean total ozone column distribution in January (1978-2008).

Results III

- Comparison of MUAM residual vertical velocity and trace gases distributions confirms realistic behaviour of modeled atmosphere
- From roughly 35°N we can see evidence (N2O, O3, H2O) of the enhanced branch of BDC above NP/EA region reaching lowest levels around 140°E (compare with location of IGW activity hotspot)
- Tropopause (chemical) located at lower altitudes above NP/EA region than on other longitudes as suggested by CO fields. Local maxima of CO concentration around 15 km altitude between 27.5 and 37.5°N and around 130°E signs of STE?

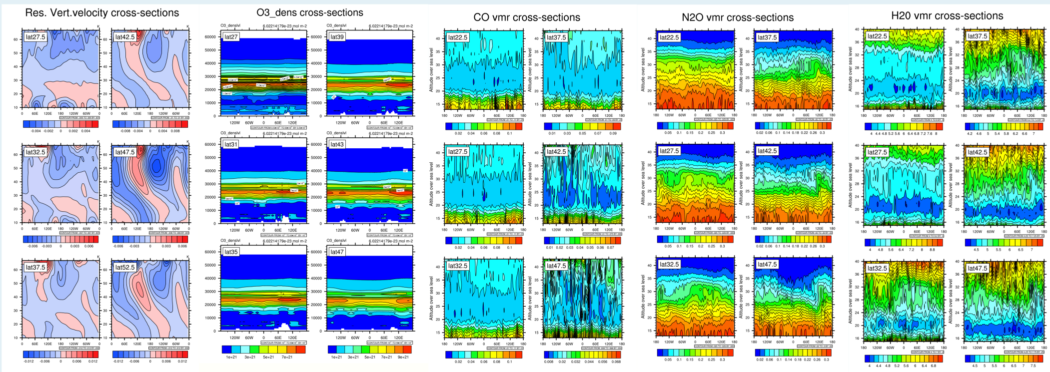

Fig. 7: Zonal cross-sections at latitudes around 35°N of MUAM residual vertical velocity in November, O3 mole content in atmospheric layer and volume mixing ratios of N2O, H2O and CO for November 2009.

Summary and conclusions

- Using GPS RO data high IGW potential energy values were find. Static and dynamic stability indicators suggestive of massive wave breaking in this region (Submitted to ACP).
- 2D E-P flux diagnostics of MUAM runs reveals enhanced equatorward and poleward propagation of planetary waves, if the IGW hotspot area is included – possible consequences for STE and vortex dynamics.
- Distributions of gases and 3D analysis of MUAM runs are pointing to robust downwelling of equatorial air masses (enhanced branch of Brewer-Dobson circulation) reaching deeper in the NP/EA region stratosphere than elsewhere. The causality is unclear - product of wave mean flow interactions and induced residual circulation in 3D.

REFERENCES:
Demirhan Bari, D., Gabriel, A., Körnich, H., & Peters, D. W. H. (2013). The effect of zonal asymmetries in the Brewer-Dobson circulation on ozone and water vapor distributions in the northern middle atmosphere. Journal of Geophysical Research: Atmospheres, 118(9), 3447-3466.
Ern, M., Preusse, P., Gille, J. C., Hepplewhite, C. L., Mlynczak, M. G., Russell, J. M., and Riese, M.: Implications for atmospheric dynamics derived from global observations of gravity wave momentum flux in stratosphere and mesosphere, J. Geophys. Res.-Atmos., 116, D19107, doi:10.1029/2011JD015821, 2011.
Garcia, R. R. and Randel,W. J.: Acceleration of the Brewer-Dobson circulation due to increases in greenhouse gases, J. Atmos. Sci., 65, 2731–2739, 2008.
Kinoshita, T., & Sato, K. (2013). A Formulation of Three-Dimensional Residual Mean Flow Applicable Both to Inertia-Gravity Waves and to Rossby Waves. Journal of the Atmospheric Sciences, 70(6), 1577-1602.
Marshall, A. G. and Scaife, A. A.: Impact of the QBO on surface winter climate, J. Geophys. Res.-Atmos., 114, D18110, doi:10.1029/2009JD011737, 2009.
McDonald, A. J., B. Tan, and X. Chu (2010), Role of gravity waves in the spatial and temporal variability of stratospheric temperature measured by COSMIC/FORMOSAT3 and Rayleigh lidar observations, J. Geophys. Res., 115, D19128, doi:10.1029/2009JD013658.
Šácha, P., Foelsche, U., & Pišoft, P. (2014). Atmos. Meas. Tech., 7, 4123-4132, doi:10.5194/amt-7-4123-2014, 2014.
Senft, D. C., & Gardner, C. S. (1991). Seasonal variability of gravity wave activity and spectra in the mesopause region at Urbana. Journal of Geophysical Research: Atmospheres (1984–2012), 96(D9), 17229-17264.
Wilson, R., Chanin, M. L., & Hauchecorne, A. (1991). Gravity waves in the middle atmosphere observed by Rayleigh lidar: 2. Climatology. Journal of Geophysical Research: Atmospheres (1984–2012), 96(D3), 5169-5183.

ACKNOWLEDGEMENTS.:
The study was supported by the Charles University in Prague, project GA UK No 108313, by the Aktion program, by the grant no. SVV-2014-26096, and by the Austrian Science Fund (FWF; BENCHCLIM project P22293-N21. UCAR/CDAAC (Boulder, CO, USA) is acknowledged for the provision RO data. Finally we thank Andrea K. Steiner (WEGC, University of Graz) for fruitful discussions.